Single-Layer Low-Profile Wideband Antenna Based on Non-Uniform Radiating Elements

Thai Nguyen-Dinh, Anh Nguyen-Quang, Hoang Nguyen-Huy, and Niamat Hussain

***Abstract*—This paper presents a single-layer low-profile antenna with wideband operation based on non-uniform radiating elements. The antenna is first designed with four square patches with center excitation. Then, multiple patches with different dimensions are positioned on both sides to produce two adjacent resonances in the high frequency. Accordingly, wideband operation with single layer configuration can be obtained. The final antenna has overall dimensions of $1.04\,\lambda \times 0.61\,\lambda \times 0.02\,\lambda$ at 5.2 GHz. The measurement on the fabricated antenna demonstrate wideband operation of 15.4%, ranging from 4.8 to 5.6 GHz. Across this band, the realized gain remains above 5.0 dBi with a peak of 7.9 dBi. Furthermore, the antenna maintains stable radiation patterns, and the front-to-back ratio (FBR) consistently exceeds 16 dB. Compared with existing single-layer wideband designs, the proposed antenna offers the lowest profile while providing a well-balanced combination of bandwidth, gain, and FBR.**

Link to graphical and video abstracts, and to code:
https://latamt.ieeer9.org/index.php/transactions/article/view/10613

***Index Terms*—Compact, single layer, wideband, non-uniform.**

I. Introduction

THE demand for single-layer wideband patch antennas in the C-band is rising with the growth of sub-6-GHz 5G, Wi-Fi 6E/7, and compact Internet of Thing (IoT) systems. These applications require wide impedance bandwidth, stable gain, and low-profile integration, which single-layer designs provide with lower cost and reduced fabrication complexity. As wireless systems expand within the 4–8 GHz range, efficient single-layer wideband patch antennas have become essential solutions for next-generation communication platforms.

Monopole and slotted antennas are commonly employed to achieve wideband operation using a simple single-layer configuration [1]–[5]. However, these structures typically exhibit omnidirectional radiation patterns with inherently low gain, and their integration into directional or high-performance systems is consequently limited. Microstrip patch antennas are widely used in modern wireless communication systems due to their low profile, low cost and ease of integration. However, conventional patch antennas inherently support only a single resonant mode, resulting in narrow bandwidth [6], [7], which is typically smaller than 3%. Consequently, extensive research has been devoted to enhancing the bandwidth of microstrip patch antennas.

Multi-layer architectures are widely employed to enhance the bandwidth of patch antennas. Wideband operation has been achieved through stacked-patch configurations [8], [9] and proximity-coupled feeding techniques [10]–[12]. Metasurface (MS)-based antennas also offer an effective approach for bandwidth improvement [13]–[15]. However, these designs often involve complex fabrication procedures and stringent layer-alignment requirements, which increase manufacturing difficulty and cost.

Single-layer configurations remain highly attractive for achieving simple, low-profile antenna designs. Several single-layer MS-based antennas have been reported [16]–[19]; however, these structures are typically excited through a slotted ground, which leads to increased back radiation. In contrast, single-layer patch antennas employing probe feeding help suppress back lobe radiation. Studies in [20]–[25] have demonstrated single-layer patch designs achieving operating bandwidths below 10% by introducing perturbations on the patch to excite adjacent resonances. Improved bandwidth performance has been reported in [26]–[30], where very thick substrates or parasitic elements are incorporated to enhance impedance bandwidth. Although wideband performance can be achieved in these designs, several critical drawbacks remain, including large physical size and high profile. While some structures offer very wide impedance bandwidth, they often suffer from low front-to-back ratio (FBR) and unstable radiation patterns across the operating band.

This paper presents a single-layer wideband antenna. The main contributions of this work are summarized as follows:

- A single-layer wideband patch antenna is introduced using non-uniform radiating elements to generate two closely spaced resonances, enabling wideband performance without multilayer complexity.
- A low-profile configuration of only $0.02\,\lambda$ is achieved, representing one of the thinnest profiles reported among single-layer wideband antennas in this frequency range.
- A well-balanced performance is obtained, including wide impedance bandwidth, stable radiation patterns, and a consistently high FBR.
- A fabricated prototype validates the proposed concept, demonstrating practical feasibility and suitability for modern wireless communication systems.

The antenna is first investigated using Characteristic Mode Analysis (CMA) in Section II. Section III presents the design

The associate editor coordinating the review of this manuscript and approving it for publication was Roberto S. Murphy (*Corresponding author: Thai Nguyen-Dinh*).

Thai Nguyen-Dinh, A. Nguyen-Quang, and H. Nguyen-Huy are with the Faculty of Electrical and Electronic Engineering, PHENIKAA School of Engineering, PHENIKAA University, Yen Nghia, Ha Dong, Hanoi 12116, Vietnam (e-mails: thai.nguyendinh@phenikaa-uni.edu.vn, 24108391@st.phenikaa-uni.edu.vn, and hoang.nguyenhuy@phenikaa-uni.edu.vn).

N. Hussain is with the James Watt School of Engineering, University of Glasgow, Scotland, United Kingdom (e-mail: niamat.hussain@glasgow.ac.uk).

evolution toward the final realization. The measured results are then discussed in Section IV. Finally, Section V provides a comparison with existing single-layer wideband patch antennas.

II. Antenna Design with Characteristic Mode Analysis

For better understanding the wideband performance, the Characteristic Mode Analysis (CMA) is employed to investigate the operation characteristic of the proposed design. According to [31]–[33], CMA can predict potential operating modes for arbitrarily shaped conducting bodies. Here, the narrow band and wideband antennas are considered, as shown in Fig. 1.

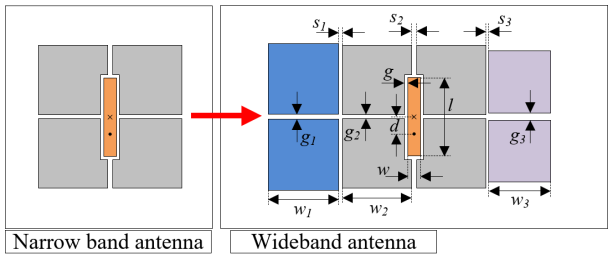

Fig. 1. Geometry of narrow and wideband antennas.

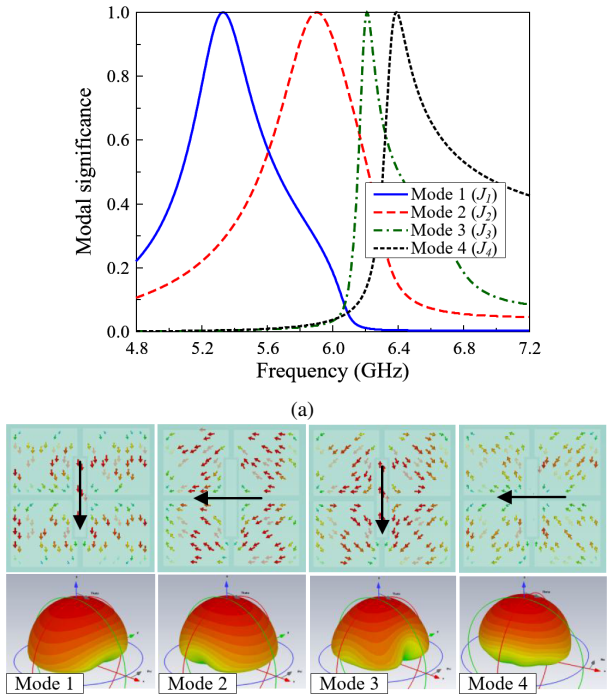

Fig. 2. CMA on the narrow band antenna. (a) modal significance, (b) surface current and far-field patterns.

Antenna with narrow band operation is first considered and the Characteristic Mode Analysis (CMA) results on this structure are indicated in Fig. 2. The square patch has a dimension of about half-wavelength at the desired frequency band. Noted that only modes with broadside radiation patterns are shown to avoid confusion. According to the CMA, mode with modal significance of approximately 1 shows potential to radiate at that frequency. Here, four resonances at 5.3, 5.9, 6.2, and 6.4 GHz respectively are potential to radiate by this design. The first mode J_1 occurs at the lowest frequency range of 5.3 GHz with current distribution along the vertical direction. The second mode J_2 at 5.9 GHz has current flowing in the horizontal direction. Higher modes J_3 and J_4 occur in higher frequency range of 6.2 and 6.4 GHz and their currents flow in vertical and horizontal directions, respectively. To achieve wideband performance, the modes J_2 and J_4 are chosen because they have similar current distributions, which are in the horizontal direction. To lower these frequencies, additional patches are utilized. These additional patches are positioned on both sides of the narrow band antenna, and they contribute to extending the electrical length.

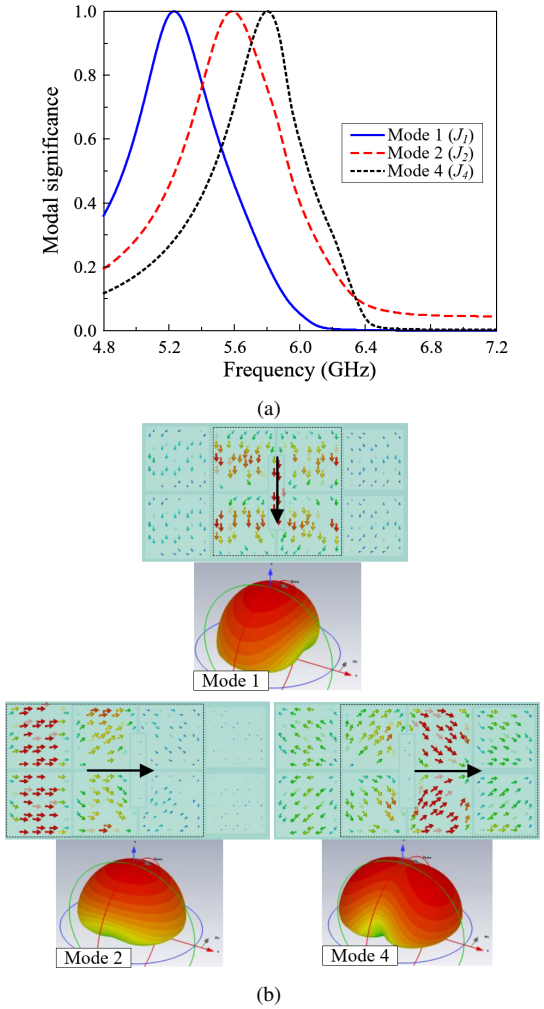

Fig. 3. CMA on the wideband antenna. (a) modal significance, (b) surface current and far-field patterns.

Characteristic Mode Analysis (CMA) on the wideband antenna is carried out, and the results are depicted in Fig. 3. It is noted that higher modes with broadside radiation that occur in higher frequency range are ignored since they cannot help to extend the operating bandwidth. It can be seen obviously that modes J_2 and J_4 move closer to mode J_1. Here, mode J_2

(5.6 GHz) are highly distributed on 6 patches on the left side, while mode J_4 (5.9 GHz) are distributed on the right side.

III. Antenna Design and Performance

A. Antenna Design

To validate the effectiveness of the CMA approach, Fig. 4 shows the design evolution of the proposed single-layer wideband antenna. Three different structures are considered for better understanding the operation mechanism of the proposed antenna. All structures are printed on the top layer of a Taconic RF-35 substrate ($\varepsilon_r = 3.5$, $\tan\delta = 0.003$) and directly excited through a 50-Ω SMA connector.

Design-1 with four patches is first considered. Then, Design-2 is introduced with two square patches on the left side. Finally, two additional patches are positioned on the right side, designated as Design-3. The antenna is optimized to achieve the best possible performance in terms of reflection coefficient and broadside gain across the widest attainable frequency band. Full-wave electromagnetic simulations are conducted using Ansys High Frequency Structure Simulator (HFSS) to characterize the antenna's operational behaviour. The optimized design parameters for each design can be found in Table I. Noted that the dimensions of the patches must be adjusted at each stage. The reason behind this is that when additional patches are positioned in proximity to the four center patches. The gaps between them will directly affect the capacitance of the first resonance producing by the four center patches. Similar when positioning more patches on the left side. Thus, the dimensions of the patches should be varied at each stage.

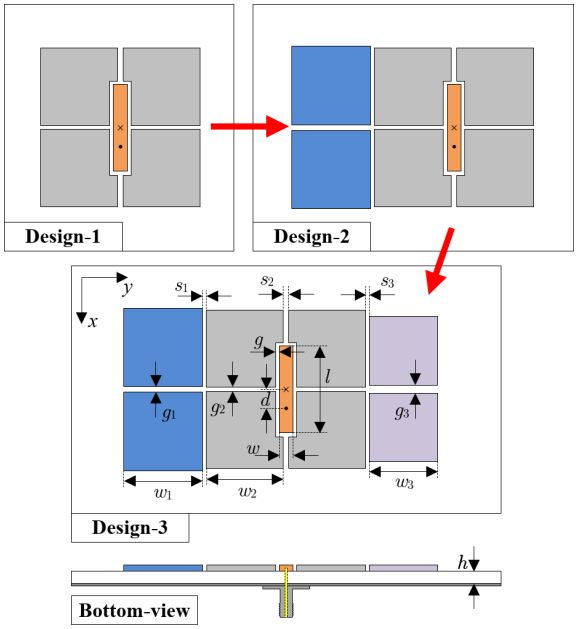

Fig. 4. Geometrical configuration of the single-layer wideband antenna.

B. Antenna Performance

The simulated reflection coefficients of different antennas are depicted in Fig. 5. As shown, the impedance bandwidth

TABLE I
Optimized Design Parameters of Different Antennas (unit: mm)

Parameter	Design-1	Design-2	Design-3
L_s	60	60	60
W_s	35	35	35
l	14.6	14.6	14.6
w	2.0	2.8	2.4
d	2.6	3.9	3.9
g	0.5	0.4	0.35
$(w_1; g_1; s_1)$	–	12.8; 0.90; 0.65	12.8; 0.65; 0.90
$(w_2; g_2; s_2)$	12.5; 1.00; 1.00	12.6; 0.70; 0.70	12.6; 0.70; 0.70
$(w_3; g_3; s_3)$	–	–	12.0; 0.65; 1.35

gradually increases from Design-1 to Design-3. Design-1 has one resonance around 5.1 GHz and the simulated −10 dB $|S_{11}|$ bandwidth ranges from 4.94 to 5.24 GHz, corresponding to about 5.9%. Wider bandwidth can be obtained for Design-2 with one additional resonance around 5.3 GHz. The simulated operating bandwidth of Design-2 is approximately 11.4% (4.82–5.40 GHz). The final antenna, Design-3, achieves the best performance with three adjacent resonances in the $|S_{11}|$ profile. This antenna attains an impedance bandwidth spanning from 4.76 to 5.68 GHz under the criterion of $|S_{11}|$ less than −10 dB, corresponding to a fractional bandwidth of approximately 17.6%.

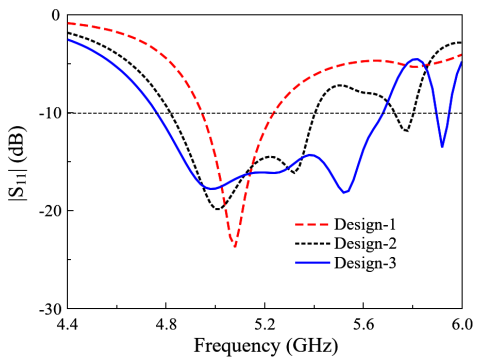

Fig. 5. Simulated reflection coefficient of different antennas.

C. Antenna Operation Characteristics

1) Design-1: Firstly, Design-1 operation characteristic is investigated. This antenna consists of four patches and capacitively fed by the rectangular patch located at the center. It is noted that the use of multiple patches and this feeding configuration provide a flexibility in tuning the operating frequency band of the antenna. For demonstration, Fig. 6 shows the simulated $|S_{11}|$ for different patch's size, w_2. It can be seen obviously that increasing w_2 results in longer electrical length, and then lower operating frequency. In terms of feeding mechanism, this structure utilizes the capacitive feeding method. Therefore, tuning the gap between the excited center patch and the radiating patches can affect the resonant frequency. As demonstrated in Fig. 7, smaller gap results in larger capacitance, which contributes to lower the resonance of the antenna.

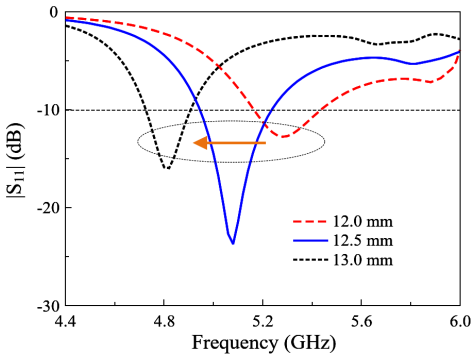

Fig. 6. Simulated $|S_{11}|$ of Design-1 for different patch's size, w_2.

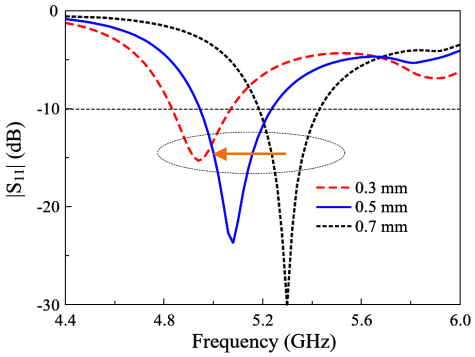

Fig. 7. Simulated $|S_{11}|$ of Design-1 for different gap's size, s.

2) Design-2: Due to the limitation in operating bandwidth of Design-1, additional patches are added to Design-2. These patches are utilized to produce adjacent resonance in higher frequency range. For better demonstration the role of the additional patches, Fig. 8 shows the simulated $|S_{11}|$ against the variations of w_1. Obviously, changing this parameter only has strong effect on the higher resonance, while the lower resonance is almost stable. Larger patch's size results and longer electrical size, and hence lower operating frequency. The optimized value of w_2 is chosen about 12.6 mm, in which one resonance around 5.3 GHz is produced. Accordingly, wideband impedance bandwidth from 4.82 to 5.40 GHz (11.4%) can be achieved.

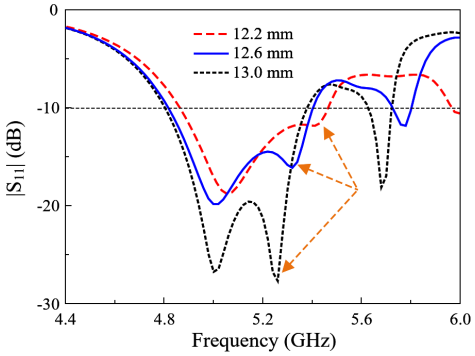

Fig. 8. Simulated $|S_{11}|$ of Design-2 for different patch's size, w_1.

3) Design-3: Further bandwidth enhancement when more patches are introduced on the right side of the antenna, Design-3. Similar to the mechanism discussed in Subsection 3c, these patches are utilized to produce additional band in the higher frequency range. This is confirmed by observing the simulated results shown in Fig. 9, which studies the $|S_{11}|$ behavior for different sizes of these additional patches, w_3. As seen clearly, changing this parameter strongly affects the highest band, while the others are remained unchanged. Increasing w_3 from 11.6 mm makes the highest resonance shift from 5.66 to 5.42 GHz. With $w_3 = 12$ mm, the antenna achieves the best performance with three resonances at 4.96, 5.24, and 5.52 GHz, respectively. The widest impedance bandwidth is from 4.76 to 5.68 GHz, equivalent to about 17.6%.

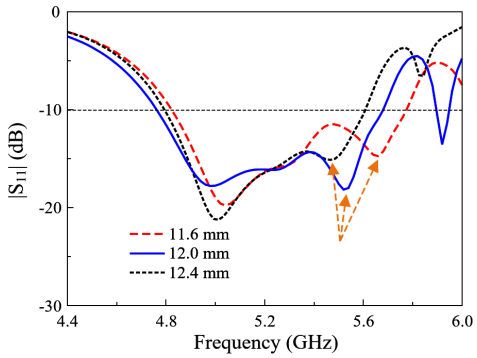

Fig. 9. Simulated $|S_{11}|$ of Design-3 for different patch's size, w_3.

To verify the function of each patch in the operation principle of the proposed antenna, the simulated surface current distributions at three different frequencies are considered and depicted in Fig. 10. At 4.96 GHz, the surface currents are predominantly concentrated on the four central patches, indicating their dominance in the lower-band resonance. As the frequency increases to 5.24 GHz, the current shifts toward the left-side patches, signifying the excitation of a higher resonance. At 5.52 GHz, the current becomes more evenly distributed across the entire array, revealing the activation of an additional adjacent resonance. These distinct current patterns across the three frequencies verify that the proposed structure supports multiple closely spaced resonant modes, which collectively produce the measured wideband performance.

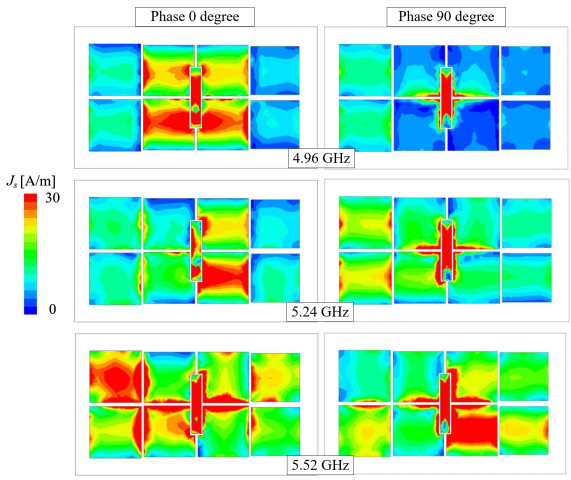

Fig. 10. Simulated current distributions of the proposed antenna.

IV. Measurement Results

The proposed concept is validated by measurement implemented on a fabricated antenna prototype, as shown in Fig. 11. The reflection coefficient is measured using an N5242A Vector Network Analyzer depicted in Fig. 12. Meanwhile, the far-field radiation characteristics are evaluated in an anechoic chamber. Overall, the measured results show good agreement with the simulations. Minor discrepancies can be attributed to fabrication tolerances and slight misalignments during the measurement setup. Noted that the tolerance in PCB processing is quite small to the gap dimensions, which have just minor effect on the measured data.

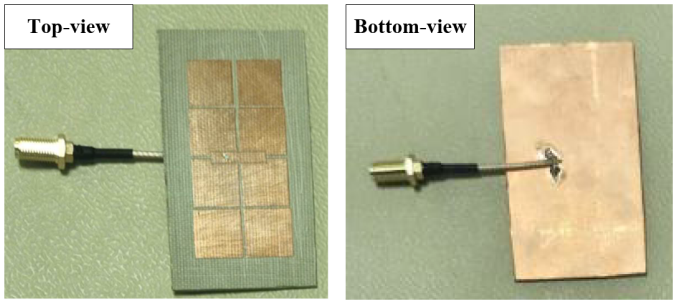

Fig. 11. Top-view and bottom-view of the fabricated antenna prototype.

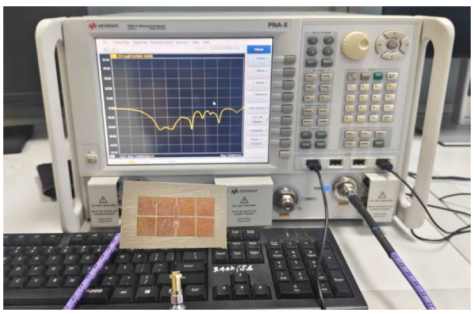

Fig. 12. Measurement with the VNA of the fabricated antenna prototype.

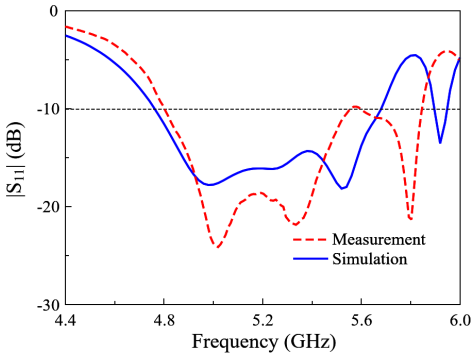

Fig. 13. Simulated and measured $|S_{11}|$ results of the proposed antenna.

The simulated and measured reflection coefficient of the proposed antenna is presented in Fig. 13. It can be seen that the measured data shows good matching performance in the frequency range from 4.8 to 5.6 GHz (15.4%). This band is just slightly smaller than the simulated band, ranging from 4.76 to 5.68 GHz.

Fig. 14 shows the simulated and measured gain in the forward and backward directions of the proposed antenna. Similar to the consistency between simulation and measurement of reflection coefficient, both measured and simulated gain curves are quite similar. In the impedance bandwidth, the broadside gain varies from 5.0 to 7.9 dBi. Meanwhile, the FBR defined by the gain difference between the main lobe and back lobe is always higher than 16 dB entire the operating bandwidth. The simulated radiation efficiency also indicates that the proposed antenna can achieve high radiation efficiency of better than 90% across the operating bandwidth.

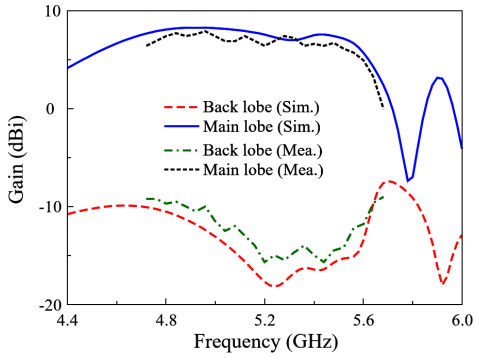

Fig. 14. Simulated and measured gain of the proposed antenna.

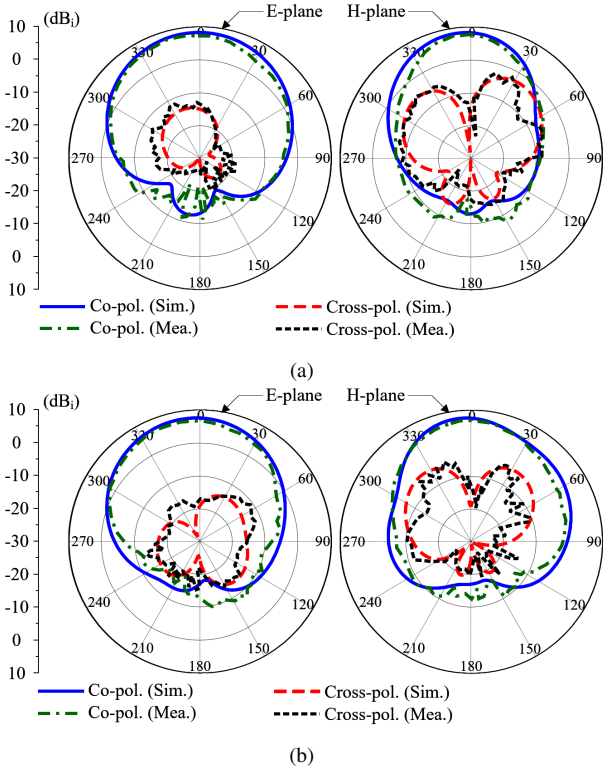

Fig. 15. Simulated and measured gain radiation patterns of the proposed antenna at (a) 5.0 GHz and (b) 5.4 GHz

Fig. 15 plots the simulated and measured gain radiation patterns of the proposed antenna. Here, the co-polarization

TABLE II
PERFORMANCE COMPARISON AMONG SINGLE-LAYER WIDEBAND PATCH ANTENNAS

Ref.	Overall dimensions (λ)	Bandwidth (%)	Max. Gain (dBi)	Min. FBR (dB)
[21]	$0.87 \times 0.87 \times 0.03$	6.8	7.0	16
[22]	$1.52 \times 1.52 \times 0.04$	6.1	10.7	22
[25]	$0.52 \times 0.52 \times 0.03$	10.6	6.4	16
[26]	$0.82 \times 0.82 \times 0.09$	24.8	7.2	Not Given
[27]	$1.22 \times 1.22 \times 0.03$	20.1	9.5	17
[28]	$2.29 \times 1.43 \times 0.11$	41.9	10.5	14
[29]	$0.82 \times 0.41 \times 0.05$	13.7	8.1	10
[30]	$0.55 \times 0.46 \times 0.07$	27.1	6.4	10
Prop.	$\mathbf{1.04 \times 0.61 \times 0.02}$	**15.4**	**7.9**	**16**

and cross-polarization in two planes of x-z and y-z at two different frequencies of 5.0 and 5.4 GHz are chosen. It can be seen clearly that the antenna radiates good broadside beams at both frequencies. The polarization purity is better than 23 dB in the broadside direction.

V. PERFORMANCE COMPARISON

The performance comparison among single-layer wideband patch antennas is summarized and presented in Table II. The antenna dimensions are calculated according to the free-space wavelength at the center operating frequency. The bandwidth, gain, as well as FBR are the key parameters for comparison.

It can be seen obviously that among the antennas with low profile of less than $0.05\,\lambda$ [21], [22], [25], [29], the proposed design achieves the largest operating bandwidth. Although the design in [27] provides a broader bandwidth, its physical size is significantly larger. The antennas in [26], [28], [30] offer wider bandwidths but at the expense of increased dimensions and reduced FBR. Besides, the overall volumes of these designs are much bigger than the proposed design. Additionally, despite having large operating bandwidth in [29], the radiation patterns in high frequency region is degraded with high side-lobe level.

Overall, the proposed antenna achieves the smallest profile among comparable single-layer designs while still providing a balanced combination of wide bandwidth, stable gain, and high FBR. Its compact height enables easy integration into space-constrained platforms, and the non-uniform radiating elements effectively realize wideband operation without multilayer complexity. The strong FBR and stable radiation patterns further highlight its well-rounded electromagnetic performance.

VI. CONCLUSION

In conclusion, this work introduces a single-layer wideband patch antenna that employs non-uniform radiating elements to generate closely spaced resonances and achieve wideband operation without multilayer complexity. The proposed design attains an exceptionally low profile of $0.02\,\lambda$, making it one of the thinnest single-layer wideband antennas reported in this frequency range. Measurements confirm a well-balanced performance in terms of bandwidth, gain, radiation stability, and FBR, demonstrating the effectiveness of the design approach. The successful fabrication and validation further highlight its suitability for compact and modern wireless communication systems. Future work will explore extending this approach to polarization-agile or reconfigurable structures and adapting the concept to multiple-input-multiple-output configurations for enhanced system capacity.

REFERENCES

[1] H. Varheenmaa, P. Ylä-Oijala, A. Lehtovuori, and V. Viikari, "Wideband sub-6 ghz mimo antenna for full-screen metal rim smartphones," *IEEE Access*, vol. 11, pp. 111 888–111 896, 2023. doi: 10.1109/access.2023.3322738

[2] M. Sultana, S. M. A. Z. Chowdhury, and M. A. Alim, "Compact u-slot microstrip antenna for wi-fi 5/6: enhancing gain, bandwidth, and efficiency," *Journal on Wireless Communications and Networking*, vol. 2026, no. 1, Dec. 2025. doi: 10.1186/s13638-025-02550-0

[3] S. De and P. Sarkar, "A high gain ultra-wideband monopole antenna," *AEU - International Journal of Electronics and Communications*, vol. 69, no. 8, pp. 1113–1117, Aug. 2015. doi: 10.1016/j.aeue.2015.04.012

[4] F. Zhang, H. Zhang, Q. You, and J. Huang, "Wideband slot antenna array with stable low-sidelobe performance," *IEEE Antennas and Wireless Propagation Letters*, vol. 24, no. 5, pp. 1248–1252, May 2025. doi: 10.1109/lawp.2025.3532116

[5] H. Yuan, J. Li, Z. Zhao, Z. Wang, M. Lodi, G. Gugliandolo, N. Donato, G. Crupi, L. Si, and X. Bao, "Development of a wideband slotted antenna array with low profile and low sidelobe," *Electronics*, vol. 12, no. 2, p. 278, Jan. 2023. doi: 10.3390/electronics12020278

[6] R. Garg, Ed., *Microstrip antenna design handbook*, ser. Artech House antennas and propagation library. Boston, Mass.: Artech House, 2001, includes bibliographical references and index.

[7] K. Carver and J. Mink, "Microstrip antenna technology," *IEEE Transactions on Antennas and Propagation*, vol. 29, no. 1, pp. 2–24, Jan. 1981. doi: 10.1109/tap.1981.1142523

[8] M. S. Shishkin, "Bandwidth enhancement methods analysis for high-gain stacked microstrip antenna," *Progress In Electromagnetics Research B*, vol. 107, pp. 19–31, 2024. doi: 10.2528/pierb24052703

[9] M. A. Matin, B. S. Sharif, and C. C. Tsimenidis, "Probe fed stacked patch antenna for wideband applications," *IEEE Transactions on Antennas and Propagation*, vol. 55, no. 8, pp. 2385–2388, Aug. 2007. doi: 10.1109/tap.2007.901924

[10] P. Hazdra, M. Mazanek, and J. Cermak, "Wideband rectangular microstrip patch antenna using l-probe feeding system," *RADIOENGINEERING-PRAGUE-*, vol. 16, no. 3, p. 37, 2007.

[11] C. Mak, K. Luk, K. Lee, and Y. Chow, "Experimental study of a microstrip patch antenna with an l-shaped probe," *IEEE Transactions on Antennas and Propagation*, vol. 48, no. 5, pp. 777–783, 2000. doi: 10.1109/8.855497

[12] C.-L. Mak, H. Wong, and K.-M. Luk, "High-gain and wide-band single-layer patch antenna for wireless communications," *IEEE Transactions on Vehicular Technology*, vol. 54, no. 1, pp. 33–40, Jan. 2005. doi: 10.1109/tvt.2004.838899

[13] D. Chen, W. Yang, Q. Xue, and W. Che, "Miniaturized wideband planar antenna using interembedded metasurface structure," *IEEE Transactions on Antennas and Propagation*, vol. 69, no. 5, pp. 3021–3026, May 2021. doi: 10.1109/tap.2020.3028245

[14] D. Chen, W. Yang, W. Che, and Q. Xue, "Miniaturized wideband metasurface antennas using cross-layer capacitive loading," *IEEE Antennas and Wireless Propagation Letters*, vol. 21, no. 1, pp. 19–23, Jan. 2022. doi: 10.1109/lawp.2021.3115356

[15] D. Chen, Q. Xue, W. Yang, K.-S. Chin, H. Jin, and W. Che, "A compact wideband low-profile metasurface antenna loaded with patch-via-wall structure," *IEEE Antennas and Wireless Propagation Letters*, vol. 22, no. 1, pp. 179–183, Jan. 2023. doi: 10.1109/lawp.2022.3206349
[16] S. Jiang, Z. Liu, H. Yang, and D. Sun, "A single-layer multimode metasurface antenna with a cpw-fed aperture for uwb communication applications," *Micromachines*, vol. 14, no. 2, p. 249, Jan. 2023. doi: 10.3390/mi14020249
[17] J. Wang, H. Wong, Z. Ji, and Y. Wu, "Broadband cpw-fed aperture coupled metasurface antenna," *IEEE Antennas and Wireless Propagation Letters*, vol. 18, no. 3, pp. 517–520, Mar. 2019. doi: 10.1109/lawp.2019.2895618
[18] J. d. D. Ntawangaheza, L. Sun, Z. Xie, Y. Pang, Z. Zheng, and G. Rushingabigwi, "A single-layer low-profile broadband metasurface antenna array for sub-6 ghz 5g communication systems," *IEEE Transactions on Antennas and Propagation*, vol. 69, no. 4, pp. 2061–2071, 2021. doi: 10.1109/TAP.2020.3027042
[19] H. Hamlbar Gerami, R. Kazemi, and A. E. Fathy, "Development of a metasurface-based slot antenna for 5g mimo applications with minimized cross-polarization and stable radiation patterns through mode manipulation," *Scientific Reports*, vol. 14, no. 1, Apr. 2024. doi: 10.1038/s41598-024-58794-1
[20] J.-D. Zhang, L. Zhu, Q.-S. Wu, N.-W. Liu, and W. Wu, "A compact microstrip-fed patch antenna with enhanced bandwidth and harmonic suppression," *IEEE Transactions on Antennas and Propagation*, vol. 64, no. 12, pp. 5030–5037, Dec. 2016. doi: 10.1109/tap.2016.2618539
[21] J.-U. Yoo and H.-W. Son, "A simple compact wideband microstrip antenna consisting of three staggered patches," *IEEE Antennas and Wireless Propagation Letters*, vol. 19, no. 12, pp. 2038–2042, Dec. 2020. doi: 10.1109/lawp.2020.3021491
[22] J.-F. Lin and L. Zhu, "Bandwidth and gain enhancement of patch antenna based on coupling analysis of characteristic modes," *IEEE Transactions on Antennas and Propagation*, vol. 68, no. 11, pp. 7275–7286, Nov. 2020. doi: 10.1109/tap.2020.2995426
[23] S. Xiao, Z. Shao, B.-Z. Wang, M.-T. Zhou, and M. Fujise, "Design of low-profile microstrip antenna with enhanced bandwidth and reduced size," *IEEE Transactions on Antennas and Propagation*, vol. 54, no. 5, pp. 1594–1599, May 2006. doi: 10.1109/tap.2006.874362
[24] R. Vincenti Gatti, R. Rossi, and M. Dionigi, "Single-layer line-fed broadband microstrip patch antenna on thin substrates," *Electronics*, vol. 10, no. 1, p. 37, Dec. 2020. doi: 10.3390/electronics10010037
[25] T. Dao-Duc, N. Truong-Quang, T. Le-Tuan, and H. Tran-Huy, "High front-to-back ratio metasurface antenna with single-layer and compact size for wlan applications," *PLOS One*, vol. 20, no. 5, p. e0321603, May 2025. doi: 10.1371/journal.pone.0321603
[26] K.-L. Wong and W.-H. Hsu, "A broad-band rectangular patch antenna with a pair of wide slits," *IEEE Transactions on Antennas and Propagation*, vol. 49, no. 9, pp. 1345–1347, 2001. doi: 10.1109/8.951507
[27] D. Yang, H. Zhai, C. Guo, and H. Li, "A compact single-layer wideband microstrip antenna with filtering performance," *IEEE Antennas and Wireless Propagation Letters*, vol. 19, no. 5, pp. 801–805, May 2020. doi: 10.1109/lawp.2020.2980631
[28] Y. Cao, Y. Cai, W. Cao, B. Xi, Z. Qian, T. Wu, and L. Zhu, "Broadband and high-gain microstrip patch antenna loaded with parasitic mushroom-type structure," *IEEE Antennas and Wireless Propagation Letters*, vol. 18, no. 7, pp. 1405–1409, Jul. 2019. doi: 10.1109/lawp.2019.2917909
[29] K. Gao, X. Cao, T. Li, H. Yang, S. J. Li, and J. Gao, "Wideband single-layer patch antenna with stable high gain using characteristic mode analysis," *IET Microwaves, Antennas & Propagation*, vol. 16, no. 8, pp. 537–543, May 2022. doi: 10.1049/mia2.12265
[30] S.-H. Wi, Y.-S. Lee, and J.-G. Yook, "Wideband microstrip patch antenna with u-shaped parasitic elements," *IEEE Transactions on Antennas and Propagation*, vol. 55, no. 4, pp. 1196–1199, Apr. 2007. doi: 10.1109/tap.2007.893427
[31] R. Harrington and J. Mautz, "Theory of characteristic modes for conducting bodies," *IEEE Transactions on Antennas and Propagation*, vol. 19, no. 5, pp. 622–628, 1971. doi: 10.1109/TAP.1971.1139999
[32] M. Cabedo-Fabres, E. Antonino-Daviu, A. Valero-Nogueira, and M. F. Bataller, "The theory of characteristic modes revisited: A contribution to the design of antennas for modern applications," *IEEE Antennas and Propagation Magazine*, vol. 49, no. 5, pp. 52–68, 2007. doi: 10.1109/MAP.2007.4395295
[33] H. Nguyen-Manh, G. Nguyen-Hoai, D.-P. Pham, T. Chu-Anh, and N. Quoc Dinh, "Single-layer compact circularly polarized antenna for unmanned aerial vehicle applications," *IEEE Access*, vol. 13, pp. 164 675–164 681, 2025. doi: 10.1109/ACCESS.2025.3606538

Thai Nguyen-Dinh received a B.S. degree in Communication Command at Telecommunications University, Vietnam, in 2010. He received his M.S. degree in Telecommunication Engineering from Posts and Telecommunications Institute of Technology, Vietnam in 2021. He is currently pursuing a Ph.D degree at Le Quy Don Technical University, Hanoi, Vietnam. His research interests have included reconfigurable antennas, MIMO antennas, and metamaterial-based antennas.

Anh Nguyen-Quang is currently an undergraduate student majoring in Electrical and Electronic Engineering with Faculty of Electrical and Electronic Engineering at Phenikaa School of Engineering, Phenikaa University, Hanoi, Vietnam. His research activities are focused on the design and optimization of microstrip antennas, RF circuit design, and electromagnetics.

Hoang Nguyen-Huy received the B.E. degree in Electronics and Telecommunications from the Hanoi University of Science and Technology (HUST), Hanoi, Vietnam, in 2013. He is currently a Research Assistant with the Faculty of Electrical and Electronic Engineering at Phenikaa School of Engineering, Phenikaa University, Hanoi, Vietnam. His current research interests involve the development of single-layer microstrip patch antennas and low-profile wideband structures. His research activities are centered on achieving high-performance radiation characteristics within constrained physical volumes, focusing on impedance bandwidth expansion and the integration of wideband elements into compact RF front-ends.

Niamat Hussain (Senior Member, IEEE) is a Lecturer (Assistant Professor) at the Division of Electronics and Nanoscale Engineering, James Watt School of Engineering, University of Glasgow, UK. Previously, he worked as an Assistant Professor in Intelligent Mechatronics Engineering at Sejong University, Korea (2022–2024). Dr. Niamat's research expertise spans Antenna Engineering, including mm-wave and THz antennas, metasurface and beamforming antennas; Microwave Engineering, such as wireless power transfer and Reflecting Intelligent Surfaces, and metamaterials; and Bioelectromagnetics, focusing on SAR reduction in wearable devices and the health effects of electromagnetic fields. Dr. Niamat's work has been recognized globally. He has been featured among the World's Top 2% Scientists (2021–2023) by Stanford University and received numerous other awards, including an endorsement as a UK Exceptional Talent in the field of Applied Electromagnetics, awarded to early-career world-leading innovators and scientists by the Royal Academy of Engineering under the UKBA Tier 1 program. Dr. Niamat is actively involved in professional activities, serving as an Associate Editor of the IEEE Internet of Things Journal, editorial board member for Electronics, Micromachines, IET Microwaves, Antennas, and Propagation, and guest editor for multiple prestigious journals. He is a senior member of IEEE and several professional societies, including the European Bioelectromagnetic Society, the Korean Society of Electromagnetic Engineering and Science, and a Member of the Evaluation Committee for National Research and Development Projects in South Korea. His research is dedicated to advancing technology with a strong focus on societal and environmental benefits.